Heliyon 10 (2024) e37580

Contents lists available at ScienceDirect

Heliyon

journal homepage: www.cell.com/heliyon

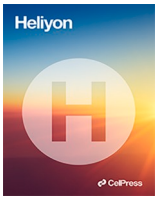

Research article

Non-invasive diagnosis of pancreatic steatosis with ultrasound images using deep learning network

Yang Sun [a,1], Li Zhang [a,1], Jian-Qiu Huang [a], Jing Su [b,**], Li-Gang Cui [a,*]

[a] Department of Ultrasound, Peking University Third Hospital, Beijing, China
[b] Department of Pathology, School of Basic Medical Science, Peking University Health Science Center, Beijing, China

ARTICLE INFO

Keywords:
Pancreatic steatosis
Type 2 diabetes mellitus
Ultrasonography
Deep learning

ABSTRACT

Objective: This study aimed to verify whether pancreatic steatosis (PS) is an independent risk factor for type 2 diabetes mellitus (T2DM). We also developed and validated a deep learning model for the diagnosis of PS using ultrasonography (US) images based on histological classifications.

Methods: In this retrospective study, we analysed data from 139 patients who underwent US imaging of the pancreas followed by pancreatic resection at our medical institution. Logistic regression analysis was employed to ascertain the independent predictors of T2DM. The diagnostic efficacy of the deep learning model for PS was assessed using receiver operating characteristic curve analysis and compared with traditional visual assessment methodology in US imaging.

Results: The incidence rate of PS in the study cohort was 64.7 %. Logistic regression analysis revealed that age ($P = 0.003$) and the presence of PS ($P = 0.048$) were independent factors associated with T2DM. The deep learning model demonstrated robust diagnostic capabilities for PS, with areas under the curve of 0.901 and 0.837, sensitivities of 0.895 and 0.920, specificities of 0.700 and 0.765, accuracies of 0.814 and 0.857, and F1-scores of 0.850 and 0.885 for the training and validation cohorts, respectively. These metrics significantly outperformed those of conventional US imaging ($P < 0.001$ and $P = 0.045$, respectively).

Conclusion: The deep learning model significantly enhanced the diagnostic accuracy of conventional ultrasound for PS detection. Its high sensitivity could facilitate widespread screening for PS in large populations, aiding in the early identification of individuals at an elevated risk for T2DM in routine clinical practice.

1. Introduction

Pancreatic steatosis (PS) refers to the excessive accumulation of fat within the pancreas [1], with an estimated prevalence in the general population between 16 % and 35 % [2–4]. Emerging studies have suggested that excess fat storage is a potential cause of beta

* Corresponding author. Department of Ultrasound, Peking University Third Hospital, 49 North Garden Rd., Haidian District, Beijing, 100191, China.
** Corresponding author. Department of Pathology, Peking University Third Hospital, 49 North Garden Rd., Haidian District, Beijing, 100191, China.
E-mail addresses: sujing@bjmu.edu.cn (J. Su), cuiligang_bysy@126.com (L.-G. Cui).
[1] These authors contributed equally to this work and should be considered joint first author.

https://doi.org/10.1016/j.heliyon.2024.e37580
Received 4 June 2024; Received in revised form 5 September 2024; Accepted 5 September 2024
Available online 6 September 2024

List of abbreviations

PS	Pancreatic steatosis
T2DM	Type 2 diabetes mellitus
US	ultrasonography
CT	computed tomography
MRI	magnetic resonance imaging
PDFF	proton density fat fraction
OR	odd ratio
BMI	body mass index
ALT	alanine aminotransferase
AST	aspartate aminotransferase
HDL-C	high-density lipoprotein cholesterol
LDL-C	low-density lipoprotein cholesterol
AUC	area under the curve
CI	confidence interval

cell dysfunction and apoptosis through lipoapoptosis, ultimately leading to type 2 diabetes mellitus (T2DM) [5,6]. Early diagnosis of PS, which includes lifestyle interventions, plays a vital role in improving beta cell function [7,8]. Consequently, developing a reliable, non-invasive, and rapid diagnostic method for PS is critical, as it could serve as a screening tool to identify populations at risk for T2DM and improve their prognosis.

Histological examination of pancreatic specimens is the gold standard for diagnosing PS and detecting fat deposits within the organ. However, given the retroperitoneal location of the pancreas, tissue sampling using surgical approaches or endoscopy is not feasible, making it impractical for routine clinical use [9]. Percutaneous tru-cut biopsy is also an applicable method in clinical practice; however, it is invasive as well.

Imaging methods such as ultrasonography (US), computed tomography (CT), and magnetic resonance imaging (MRI) are gaining importance in the diagnosis of PS. CT imaging identifies fatty deposits as a decrease in attenuation [10,11], but its use is limited owing to ionising radiation exposure, especially in adolescents, where the incidence of PS exceeds 50 % [12]. Additionally, the absence of consensus criteria for PS diagnosis on CT and challenges in defining pancreatic margins, particularly in atrophic conditions, further complicate the use of CT for this purpose [13]. Proton density fat fraction (PDFF) MRI is an advanced method for fat quantification; however, it is primarily designed for hepatic fat measurement, necessitating the optimisation of pancreatic fat quantification. The correlation between pancreatic PDFF and diabetes remains a topic of debate [14–17].

Recently, US technology has shown excellent performance in diagnosing liver steatosis, comparable to MRI, and is emerging as a reliable, non-radiative, cost-effective, and rapid method for the early diagnosis of hepatic steatosis [18]. PS, similar to hepatic steatosis, appears hyperechoic relative to the kidney on US [2]. However, diagnosing PS via US is more challenging because of the inability to simultaneously visualise the pancreas and kidneys, thus precluding a direct comparison of their echogenicity [19]. The absence of a reference standard in sonograms and the difficulty in obtaining pathological information have limited previous studies from accurately assessing the diagnostic efficiency for PS [2,19,20]. To the best of our knowledge, no studies have investigated the sensitivity and specificity of US imaging for PS compared with histology [21].

Deep learning, a subset of machine learning inspired by the human nervous system and based on artificial neural networks, offers significant advantages for analysing US images. It can identify repetitive texture patterns at the pixel or voxel level that are imperceptible to the naked eye, thereby enhancing US image analysis accuracy [21,22]. Deep learning-based US approaches have been successfully applied in hepatic steatosis evaluation [23,24], with one study demonstrating a deep learning model based on a two-dimensional convolutional neural network to accurately diagnose hepatic steatosis with high sensitivity and specificity [18]. However, the application of deep learning for the accurate diagnosis of PS from US images remains unexplored.

Therefore, the objective of our study was to confirm whether PS is an independent factor in T2DM and develop a deep learning model based on histological classification for diagnosing PS using US images.

2. Materials and methods

2.1. Study population

This retrospective study received approval from the Peking University Third Hospital review board, and the requirement for informed consent was waived. Between January 2017 and August 2022, 139 patients underwent pancreatic US and subsequent pancreatic resection at our institution. The surgeries included pancreatectomy, pylorus-preserving pancreaticoduodenectomy, Whipple operation, and enucleation. T2DM was diagnosed based on a fasting blood glucose level $\geq$7.0 mmol/L or a 2-h plasma glucose level $\geq$11.1 mmol/L following ingestion of 75 g oral glucose. Hypertension was defined as a systolic blood pressure $\geq$140 mm Hg or diastolic blood pressure $\geq$90 mm Hg. The patients' weights and heights were recorded to calculate the body mass index, computed as weight (kg) divided by height (m) squared. Prior to surgery, patients underwent blood tests, including liver function tests (alanine

aminotransferase and aspartate aminotransferase) and lipid profile (total cholesterol, high-density lipoprotein cholesterol, low-density lipoprotein cholesterol, and triglycerides). The exclusion criteria were as follows: (1) absence of non-tumorous pancreatic parenchyma for histological analysis and (2) presence of imaging artefacts impeding pancreas recognition on US. A detailed flow diagram of the study population is shown in Fig. 1.

Ultimately, 139 patients (78 men and 61 women; mean age 58.8 ± 13.4 years) were included. Clinical indications for pancreatectomy varied, including pancreatic adenocarcinoma (n = 41), pancreatic acinar cell carcinoma (n = 1), pancreatic intraductal papillary mucinous neoplasm (n = 10), pancreatic neuroendocrine tumour (n = 17), pancreatic serous cystadenoma (n = 4), pancreatic mucinous cystadenoma (n = 2), pancreatic pseudocyst (n = 2), solid pseudopapillary neoplasm (n = 17), cholangiocarcinoma (n = 13), bile duct adenoma (n = 1), choledochal cyst (n = 1), carcinoma of the ampulla of Vater (n = 19), adenoma of ampulla of Vater (n = 1), duodenal adenocarcinoma (n = 2), metastatic renal cell carcinoma (n = 3), metastatic cervical cancer (n = 1), retroperitoneal traumatic neuroma (n = 1), aggressive fibromatosis (n = 2), and gastrointestinal stromal tumour (n = 1).

2.2. Histologic analysis

A pathologist blinded to the clinical and US findings reviewed pancreatic specimens stained with haematoxylin and eosin. The pancreatic fat fraction in the non-tumorous pancreatic parenchyma was assessed on slides containing at least 1 cm^2 of tissue. The degree of PS was quantified as the ratio of intraparenchymal fat to the total pancreatic parenchyma area [25]. PS was defined as intraparenchymal fat comprising >10 % of the total pancreatic tissue [26] (Fig. 2a – d).

2.3. Patient grouping

A total of 139 patients were divided into two groups at a ratio of 7:3: Group 1 (97 patients) and Group 2 (42 patients). The initial visual diagnosis of PS was conducted, followed by calculation of their respective diagnostic efficacies. Subsequently, a deep learning-based diagnosis was performed, using patients in Group 1 as the training set and those in Group 2 as the validation set.

2.4. US image data acquisition and visual assessment

US examinations were performed using various convex array scanners. Patients were positioned supine to obtain clear grayscale images of the pancreas. Longitudinal pancreatic scans of the anterior abdominal wall were selected for consistency. PS was diagnosed by two observers with more than 5 and 10 years of experience in clinical practice who were blinded to the medical information of the examinees. The PS diagnostic criteria included pancreatic body hyperechogenicity relative to the kidneys. As previously described [2], because the pancreatic body and kidney could not be displayed in the same window, the observer first compared the differences in echogenicity between the liver and kidney and then compared the differences between the liver and pancreatic body. All participants were classified into either the PS or non–PS groups.

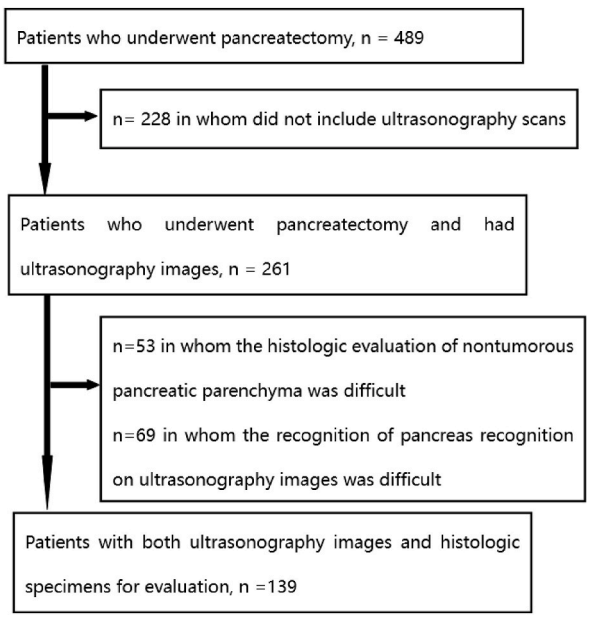

Fig. 1. Flow diagram of the study population shows selection of patients.

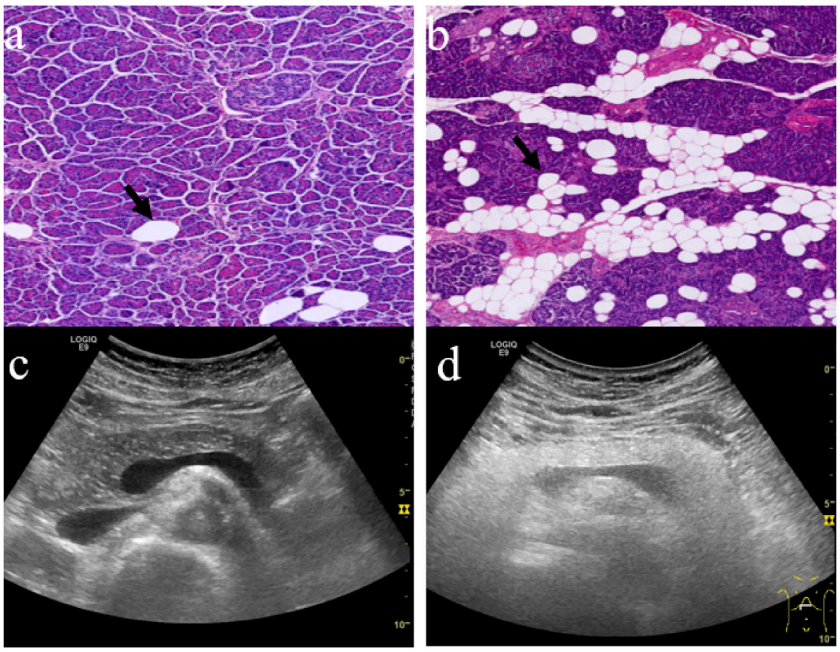

Fig. 2. (a) and (b) Histology of the human pancreas. (c) and (d) ultrasound image of pancreas. (a) Minimal adipocytes(arrow) accumulated in the pancreatic parenchyma. (b) Pancreatic steatosis. Intraparenchymal fat accounts for >10 % of the total pancreatic tissue. (c) and (d) Ultrasound images corresponding to A and B, respectively.

2.5. Deep learning network construction

In this study, we employed the transfer learning technique. The fundamental idea behind transfer learning is to adapt a pretrained model from a general image database (ImageNet, http://www.imagenet.org/) to our specific task. We fine-tuned the model using appropriate hyperparameters. Given the available data volume, we selected the well-known AlexNet architecture [27] as the backbone network. While keeping the remaining network structures unchanged, we adjusted only the output layer to suit the requirements of our task with a small sample size.

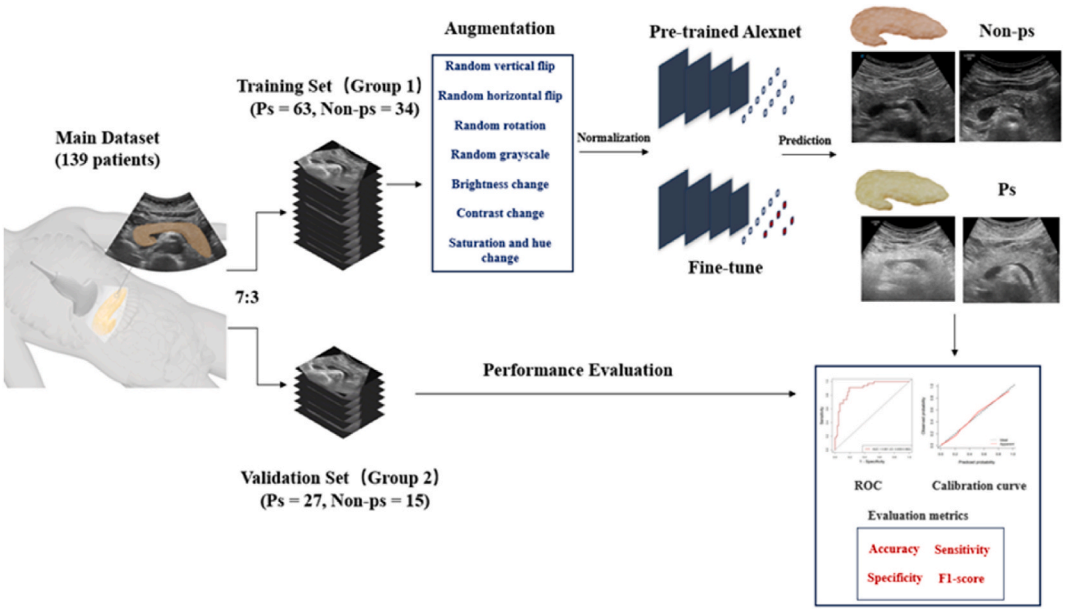

Fig. 3. Schematic diagram of the development of a deep learning network for diagnosing PS.

2.6. Data amplification and hyperparameter determination

Data augmentation techniques were employed to expand the dataset (Fig. 3). The training set was used to train the deep learning network model, update the pre-training parameters, and fine-tune the hyperparameters based on the performance. The ultrasound images were resized to 512 × 512 pixels and normalised. The optimal hyperparameters included a batch size of 64, 100 epochs, and a learning rate of 0.001. The Adam optimiser was used, with Dropout implemented in the AlexNet architecture to mitigate overfitting. The loss function was cross-entropy.

2.7. Statistical analysis

The Shapiro–Wilk test was used to assess continuous data distribution. Normal and skewed data were evaluated utilising the *t*-test and Mann–Whitney *U* test, respectively. Univariate and multivariate logistic regression analyses were employed to determine the independent risk factors for T2DM. The diagnostic performance of conventional US in the visual assessment of PS was assessed through the area under the receiver operating characteristic curve (AUC), accuracy, sensitivity, and specificity. The deep learning model construction, training, and validation were performed using the PyTorch framework (version 1.13.0) and Python (version 3.9). The hardware specifications included an Intel Core i9-10900K CPU, Nvidia RTX 3090 GPU, and Kingston DDR4-3600 with 32 GB RAM. The performance of the deep learning model was evaluated using AUC, accuracy, sensitivity, specificity, and F1-score. Cohen's kappa test was utilised to evaluate observer consistency in the PS diagnosis. The AUCs were compared using Delong's test between conventional US and the deep learning model performance.

3. Results

3.1. Baseline data of study patients

Our study comprised 139 participants. Histological analysis revealed that 64.7 % of the patients had PS. Hypertension was present in 39.5 % of patients, while 31.7 % were diagnosed with T2DM (Table 1). Logistic regression analysis was used to assess the impact of clinical variables on the risk of T2DM. After adjusting for hypertension, multivariate logistic regression analysis indicated that age ($P = 0.003$) and PS ($P = 0.048$) were significant independent risk factors for T2DM (Table 2).

3.2. Diagnostic performance of conventional US for visual assessment of PS

The agreement between the observers for the diagnosis of PS was excellent, with a kappa value of 0.914 ($P < 0.001$). The diagnostic capability of US for PS based on histological findings was quantified using AUC. In Groups 1 and 2, the ability of conventional US to diagnose PS was average, with AUC of 0.616 (95 % confidence interval [CI]: 0.512–0.713), and 0.737 (95 % CI: 0.578–0.861), respectively. Table 3 and Fig. 4a summarise the performance of conventional US.

3.3. Diagnostic performance of deep learning for evaluating PS

The deep learning model designed for the automatic diagnosis of pancreatic conditions showed high discriminatory ability. In the training set, the model's performance metrics were outstanding, with an AUC of 0.901 (95 % CI: 0.839 to 0.962), a sensitivity of 0.895, a specificity of 0.700, accuracy of 0.814, and an F1-score of 0.850 (Table 3 and Fig. 4b).

Upon evaluation using the validation dataset, the model sustained strong performance, exhibiting an AUC of 0.837 (95 % CI: 0.708 to 0.966), a sensitivity of 0.920, a specificity of 0.765, an accuracy of 0.857, and an F1-score of 0.885 (Table 3 and Fig. 4b).

Table 1
Baseline characteristics of all participants.

Characteristic	Value
Age (years)	58.8 ± 13.4(n = 139)
Gender, males/females (n)	78/61
BMI (kg/m^2)	24.0 (21.3, 26.6) (n = 133)
ALT (U/l)	25.0(15.0, 39.0) (n = 135)
AST (U/l)	22.0(17.0, 35.0) (n = 135)
Total cholesterol(mmol/L)	4.5(3.9, 5.4) (n = 132)
Triglycerides(mmol/L)	1.3(1.0, 1.8) (n = 132)
HDL-C(mmol/L)	1.0(0.8, 1.3) (n = 132)
LDL-C(mmol/L)	2.9(2.4, 3.5) (n = 132)
Hypertension, n (%)	55(39.5) (n = 139)
T2DM, n (%)	44 (31.7) (n = 139)
PS, n (%)	90(64.7) (n = 139)

Note: ALT, alanine aminotransferase; AST, aspartate aminotransferase; HDL-C, high-density lipoprotein cholesterol; LDL-C, low-density lipoprotein cholesterol; T2DM, Type 2 diabetes mellitus; PS, pancreatic steatosis.

Table 2
Logistic regression analysis showing factors associated with T2DM.

	Univariate		Multivariate	
	OR	P	OR	P
Age	1.056 (1.022, 1.090)	0.001	1.053 (1.018, 1.089)	0.003
Gender	1.489 (0.713, 3.111)	0.290		
BMI	0.930 (0.998, 1.036)	0.836		
ALT	0.996(0.989, 1.004)	0.341		
AST	0.995 (0.983, 1.007)	0.402		
Total cholesterol	1.110 (0.835, 1.475)	0.474		
Triglycerides	0.969 (0.680, 1.379)	0.859		
HDL-C	0.791 (0.349, 1.879)	0.573		
LDL-C	1.060 (0.771, 1.456)	0.721		
PS	3.261 (1.369, 7.769)	0.008	2.491 (1.008, 6.155)	0.048
Hypertension	2.300 (1.104, 4.793)	0.026		

Note: OR, odd ratio; BMI, body mass index; ALT, alanine aminotransferase; AST, aspartate aminotransferase; HDL-C, high-density lipoprotein cholesterol; LDL-C, low-density lipoprotein cholesterol; T2DM, Type 2 diabetes mellitus; PS, pancreatic steatosis.

When comparing the diagnostic performance for PS based on histology, the deep learning model outperformed conventional US in both the training and validation datasets (0.901 [95 % CI: 0.839 to 0.962] vs. 0.616 [95 % CI: 0.512 to 0.713]; 0.837 [95 % CI: 0.708 to 0.966] vs. 0.737 [95 % CI: 0.578 to 0.861]; $P < 0.001$ and $P = 0.045$, respectively; Fig. 5a, b).

4. Discussion

Our study identified age and PS as independent risk factors for T2DM. Furthermore, we developed a deep learning model to diagnose PS that yielded the highest AUCs of 0.901 and 0.837 in the training and validation groups, respectively. These results highlight the promising sensitivity of the model in diagnosing PS and its potential as a screening tool to identify populations at risk for T2DM.

Recent studies have suggested a close link between PS and T2DM. However, this conclusion remains controversial [6]. This controversy may stem from difficulties in obtaining pancreatic tissue samples, small sample sizes, and imperfections in imaging methods for diagnosing PS [1,10,11]. These discrepancies underscore the need for further research and highlight the importance of our histological approach, which validates PS as an independent risk factor of T2DM. The observed incidence of PS in our cohort was 64.7 %, which was markedly higher than the 16 %–35 % reported in the literature [26]. This discrepancy could be attributed to the advanced age of our participants, as age is known to correlate with intrapancreatic fat deposition, particularly beyond the age of 60 [28,29]. Consequently, early screening and diagnosis are imperative for implementing timely interventions to improve outcomes in patients at high risk of T2DM.

Previous studies have described the imaging characteristics of PS using US; however, they did not address its sensitivity and specificity in relation to histology [2,20]. To the best of our knowledge, this is the first study to evaluate the diagnostic efficacy of US imaging for PS based on histology. Our deep learning model outperformed the traditional visual assessment in both the training and validation datasets, demonstrating a sensitivity similar to that of MRI examinations [19]. Notably, the deep learning model offers a more accessible and cost-effective alternative to MRI for PS diagnosis.

Our study had certain limitations. This study lacked a control group of healthy individuals as pancreatic specimens were available only from patients undergoing pancreatectomy. Moreover, the presence of pancreatic tumours may be an additional confounding factor that affects PS. To maintain consistency, we primarily chose US images of the pancreatic body, which may have overlooked the differences in pancreatic fat deposition in other parts. The retrospective nature of the study introduced the possibility of selection bias, and the sample size was relatively small. Because this was a retrospective study, we could not perform quality control during the inspection. Furthermore, external validation in a separate centre using the same methodology is required to corroborate our findings.

In conclusion, our study not only corroborates PS as an independent risk factor for T2DM but also introduces a high-performance deep learning model based on US imaging for PS diagnosis. This model has the potential to facilitate widespread screening and aid in the identification of individuals at high risk of T2DM in routine clinical practice.

Data availability statement

All data derived from this study are presented in the text.

Ethics statement

The approval of this study was from Peking University Third Hospital Medical Science Research Ethics Committee (M2023510).

Funding

This study has received funding by National Natural Science Foundation of China (82102071), and Natural Science Foundation of

Table 3
Performance of visual assessment and the deep learning model in diagnosing pancreatic steatosis.

Method	Training set (Group 1)					Validation set (Group 2)				
	Accuracy	AUC (95 % CI)	Sensitivity	Specificity	F1-score	Accuracy	AUC (95 % CI)	Sensitivity	Specificity	F1-score
Visual assessment	0.598	0.616 (0.512–0.713)	0.676	0.556		0.738	0.737 (0.578–0.861)	0.733	0.741	
Deep learning	0.814	0.901 (0.839–0.962)	0.895	0.700	0.850	0.857	0.837 (0.708–0.966)	0.920	0.765	0.885

Note: AUC, area under the curve; CI, confidence interval.

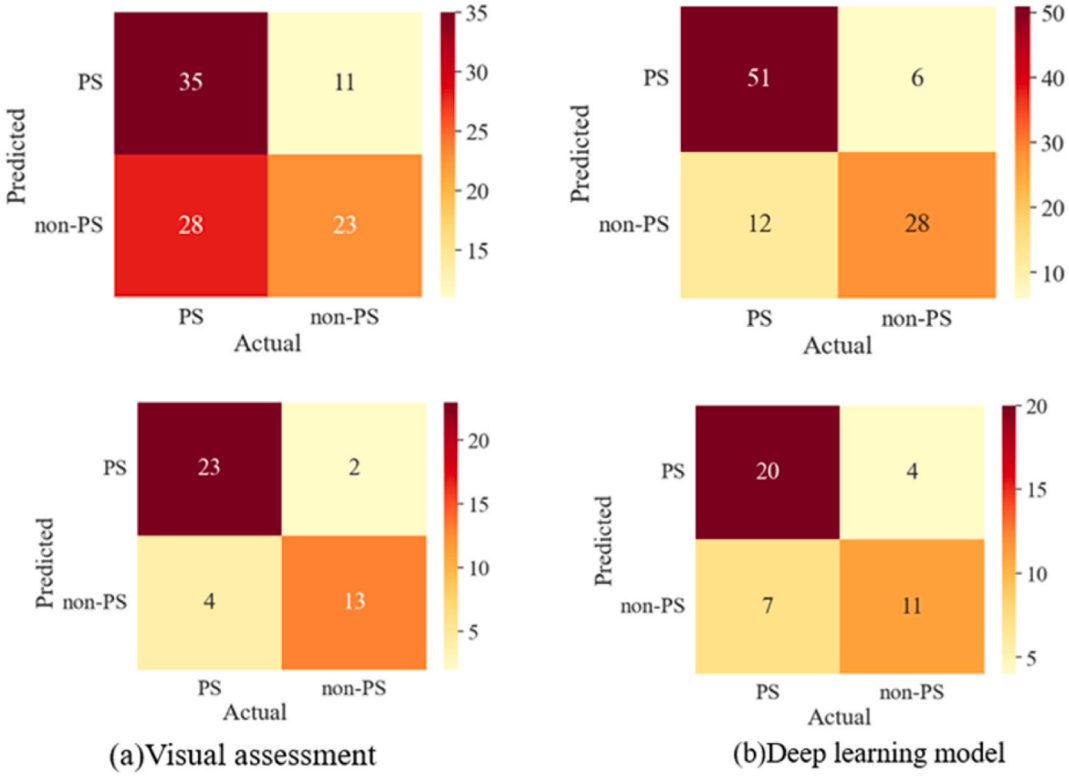

Fig. 4. Confusion matrices for classification based on visual assessment (a) and the deep learning model (b). The number of patients correctly classified are shown in the upper left and lower right corners.

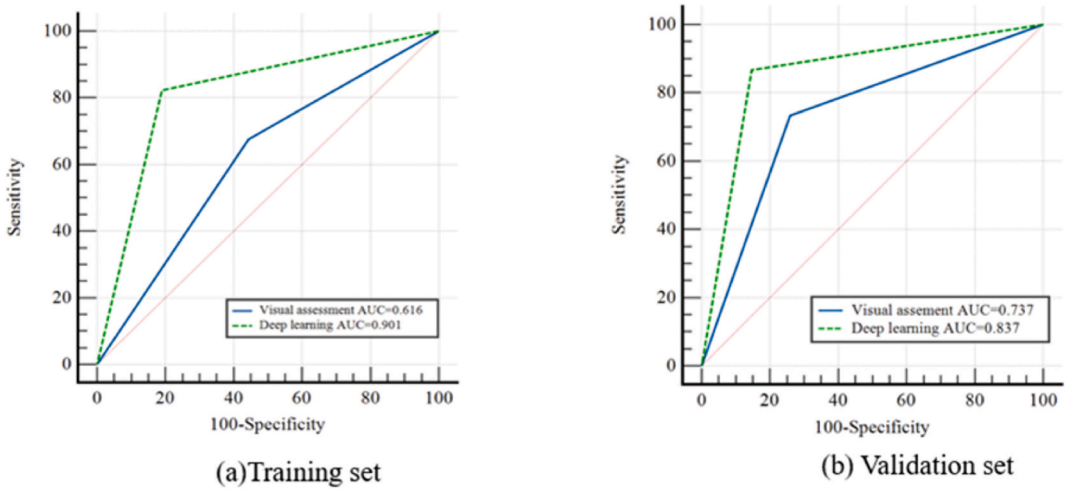

Fig. 5. Comparison of AUCs between visual assessment and the deep learning model in the (a) training set and (b) validation set.AUC, area under the curve.

Shaanxi Province (2022JM-562).

CRediT authorship contribution statement

Yang Sun: Writing – original draft, Investigation, Conceptualization. **Li Zhang:** Writing – original draft, Formal analysis. **Jian-Qiu Huang:** Writing – original draft, Investigation. **Jing Su:** Writing – original draft, Supervision. **Li-Gang Cui:** Writing – review & editing, Supervision.

Declaration of competing interest

The authors declare the following financial interests/personal relationships which may be considered as potential competing interests:Yang Sun reports financial support was provided by National Natural Science Foundation of China. Jing Su reports financial support was provided by Natural Science Foundation of Shaanxi Province. If there are other authors, they declare that they have no known competing financial interests or personal relationships that could have appeared to influence the work reported in this paper.

References

[1] M.J. Cao, W.J. Wu, J.W. Chen, et al., Quantification of ectopic fat storage in the liver and pancreas using six-point Dixon MRI and its association with insulin sensitivity and β-cell function in patients with central obesity, Eur. Radiol. 33 (12) (2023) 9213–9222.
[2] C.Y. Wang, H.Y. Ou, M.F. Chen, T.C. Chang, C.J. Chang, Enigmatic ectopic fat: prevalence of nonalcoholic fatty pancreas disease and its associated factors in a Chinese population, J. Am. Heart Assoc. 3 (1) (2014) e000297.
[3] W.S. Wong, L.H. Wong, K.W. Yeung, et al., Fatty pancreas, insulin resistance, and β-cell function: a population study using fat-water magnetic resonance imaging, Am. J. Gastroenterol. 109 (4) (2014) 589–597.
[4] S. Weng, J. Zhou, X. Chen, Y. Sun, Z. Mao, K. Chai, Prevalence and factors associated with nonalcoholic fatty pancreas disease and its severity in China, Medicine 97 (26) (2018) e11293.
[5] R. Catanzaro, B. Cuffari, A. Italia, F. Marotta, Exploring the metabolic syndrome: nonalcoholic fatty pancreas disease, World J. Gastroenterol. (34) (2016) 16.
[6] R.G. Singh, H.D. Yoon, L.M. Wu, J. Lu, L.D. Plank, M.S. Petrov, Ectopic fat accumulation in the pancreas and its clinical relevance: a systematic review, meta-analysis, and meta-regression, Metabolism: clinical and experimental 69 (2017) 1–13.
[7] L. Chen, D.J. Magliano, P.Z. Zimmet, The worldwide epidemiology of type 2 diabetes mellitus–present and future perspectives, Nat. Rev. Endocrinol. 8 (4) (2011) 228.
[8] Y. Zhao, Z. Jiang, C. Guo, New hope for type 2 diabetics: targeting insulin resistance through the immune modulation of stem cells, Autoimmun. Rev. 11 (2) (2012) 137–142.
[9] R. Taylor, A. Al-Mrabeh, S. Zhyzhneuskaya, et al., Remission of human type 2 diabetes requires decrease in liver and pancreas fat content but is dependent upon capacity for beta cell recovery, Cell Metabol. 28 (4) (2018) 547–556.
[10] M.A. Heiskanen, K.K. Motiani, A. Mari, et al., Exercise training decreases pancreatic fat content and improves beta cell function regardless of baseline glucose tolerance: a randomised controlled trial, Diabetologia 61 (8) (2018) 1817–1828.
[11] H. Yamazaki, J. Wang, M. Dohke, et al., Longitudinal association of fatty pancreas with the incidence of type-2 diabetes in lean individuals: a 6-year computed tomography-based cohort study, J. Gastroenterol. 55 (7) (2020) 712–721.
[12] H. Yamazaki, T. Tsuboya, A. Katanuma, et al., Lack of independent association between fatty pancreas and incidence of type 2 diabetes mellitus: 5-year Japanese cohort study, Diabetes Care 39 (10) (2016) 1677–1683.
[13] C. Chiyanika, D.F.Y. Chan, S.C.N. Hui, et al., The relationship between pancreas steatosis and the risk of metabolic syndrome and insulin resistance in Chinese adolescents with concurrent obesity and non-alcoholic fatty liver disease, Pediatric Obesity 15 (9) (2020) e12653.
[14] N.S. Sakai, S.A. Taylor, M.D. Chouhan, Obesity, metabolic disease and the pancreas—quantitative imaging of pancreatic fat, Br. J. Radiol. 91 (1089) (2018) 20180267.
[15] K. Shingo, I. Akito, K. Yusuke, et al., Three-dimensional analysis of pancreatic fat by fat-water magnetic resonance imaging provides detailed characterization of pancreatic steatosis with improved reproducibility, PLoS One 14 (12) (2019) e0224921.
[16] I.S. Idilman, A. Tuzun, B. Savas, et al., Quantification of liver, pancreas, kidney, and vertebral body MRI-PDFF in non-alcoholic fatty liver disease, Abdom. Imag. 40 (6) (2015) 1512–1519.
[17] N.S. Patel, M.R. Peterson, D.A. Brenner, E. Heba, C. Sirlin, R. Loomba, Association between novel MRI-estimated pancreatic fat and liver histology-determined steatosis and fibrosis in non-alcoholic fatty liver disease, Aliment. Pharmacol. Ther. 37 (6) (2013) 630–639.
[18] K. Jens-Peter, B. Friederike, M. Julia, et al., Pancreatic steatosis demonstrated at mr imaging in the general population clinical relevance, Radiology 276 (1) (2015) 129–136.
[19] S.K. Jeon, J.M. Lee, I. Joo, J.H. Yoon, G. Lee, Two-dimensional convolutional neural network using quantitative US for noninvasive assessment of hepatic steatosis in NAFLD, Radiology 307 (1) (2023) e221510.
[20] J.S. Lee, S.H. Kim, D.W. Jun, et al., Clinical implications of fatty pancreas: correlations between fatty pancreas and metabolic syndrome, World J. Gastroenterol. 15 (15) (2009) 1869–1875.
[21] J. Zhou, M.-L. Li, Z. Dan-Dan, et al., The correlation between pancreatic steatosis and metabolic syndrome in a Chinese population, Pancreatology 16 (4) (2016) 578–583.
[22] B.J. Erickson, K. Panagiotis, A. Zeynettin, T.L. Kline, Machine learning for medical imaging, Radiographics 37 (2) (2017) 10.
[23] JEv Timmeren, D. Cester, S. TanadiniLang, H. Alkadhi, B. Baessler, Radiomics in medical imaging—"how-to" guide and critical reflection, Insights into Imaging 11 (1) (2020) 91.
[24] B. Micha, S. Grzegorz, S. Cezary, et al., Transfer learning with deep convolutional neural network for liver steatosis assessment in ultrasound images, Int. J. Comput. Assist. Radiol. Surg. 13 (12) (2018) 1895–1903.
[25] R. Wagner, S.S. Eckstein, H. Yamazaki, et al., Metabolic implications of pancreatic fat accumulation, Nat. Rev. Endocrinol. 18 (1) (2021) 43–54.
[26] S.Y. Kim, H. Kim, J.Y. Cho, S. Lim, H.S. Kang, Quantitative assessment of pancreatic fat by using unenhanced CT: pathologic correlation and clinical implications, Radiology 271 (1) (2014) 104.
[27] A. Krizhevsky, I. Sutskever, G.E. Hinton, Imagenet classification with deep convolutional neural networks, Commun. ACM 2017 (2017) 84–90.
[28] Y. Wang, G. Huang, S. Song, X. Pan, Y. Xia, C. Wu, Regularizing deep networks with semantic data augmentation, IEEE Trans. Pattern Anal. Mach. Intell. 44 (7) (2020) 3733–3748.
[29] R. Murakami, Y. Saisho, Y. Watanabe, et al., Pancreas fat and beta cell mass in humans with and without diabetes: an analysis in the Japanese population, J. Clin. Endocrinol. Metab. 102 (9) (2017) 3251–3260.